The Effect of Gulf Stream–induced Baroclinicity on U.S. East Coast Winter Cyclones

JOSEPH J. CIONE, SETHU RAMAN, AND LEONARD J. PIETRAFESA

Department of Marine, Earth, and Atmospheric Sciences, North Carolina State University, Raleigh, North Carolina

(Manuscript received 22 January 1992, in final form 27 May 1992)

ABSTRACT

Midlatitude cyclones develop off the Carolinas during winters and move north producing gale-force winds, ice, and heavy snow. It is believed that boundary-layer and air–sea interaction processes are very important during the development stages of these East Coast storms. The marine boundary layer (MBL) off the mid-Atlantic coastline is highly baroclinic due to the proximity of the Gulf Stream just offshore.

Typical horizontal distances between the Wilmington coastline and the western edge of the Gulf Stream vary between 90 and 250 km annually, and this distance can deviate by over 30 km within a single week. While similar weekly Gulf Stream position standard deviations also exist at Cape Hatteras, the average annual distance to the Gulf Stream frontal zone is much smaller off Cape Hatteras, normally ranging between 30 and 100 km.

This research investigates the low-level baroclinic conditions present prior to observed storm events. The examination of nine years of data on the Gulf Stream position and East Coast winter storms seems to indicate that the degree of low-level baroclinicity and modification existing prior to a cyclonic event may significantly affect the rate of cyclonic deepening off the mid-Atlantic coastline. Statistical analyses linking the observed surface-pressure decrease with both the Gulf Stream frontal location and the prestorm coastal baroclinic conditions are presented. These results quantitatively indicate that Gulf Stream–induced wintertime baroclinicity may significantly affect the regional intensification of East Coast winter cyclones.

1. Introduction

Midlatitude cyclones develop rapidly off the coast of the Carolinas throughout the winter season. These "bombs," cyclonic disturbances that experience 24-mb central-pressure decreases over 24 h, (Sanders and Gyakum 1980) often trek northward along the mid-Atlantic coastline producing gale-force winds and frozen precipitation in the form of sleet and heavy snow. It is becoming increasingly apparent that coastal marine boundary layer (MBL) and air–sea interaction processes are important in the development of these storms (Bosart et al. 1972; Bosart 1981; Rogers and Bosart 1986; Holt and Raman 1990; Huang and Raman 1990). The MBL is highly baroclinic in the region of the Carolinas due to the presence of the Gulf Stream, which is characterized by surface temperatures much warmer than those of adjacent coastal waters. During cold-air outbreak (CAO) periods, cold continental air flows offshore and quickly encounters the warm Gulf Stream environment. The relative magnitude of MBL baroclinicity in this region is a function of both the distance of the Gulf Stream front (GSF) to the shoreline as well as the severity of the CAO itself. The Gulf Stream is known to laterally meander north of Charleston, South Carolina (Pietrafesa et al. 1978; Rooney

et al. 1978; Brooks and Bane 1978). As a result, the wintertime baroclinic nature of the area can be quite variable. It is the objective of this paper to look at how the regional variability in low-level baroclinicity ultimately affects the magnitude of offshore cyclonic intensification within our study domain.

2. Data

In order to be objective and to consider only the effects of MBL baroclinicity directly associated with the presence of the Gulf Stream off the Carolinas and Virginia, a parallelogram-shaped area between the latitudes 38° and 32°N and longitudes 77° and 71°W was chosen as our storm domain (Fig. 1). This region was selected so that storms entering this area would be in a highly variable baroclinic zone caused by the lateral meanders of the Gulf Stream. All cyclonically oriented, closed circulations at the surface were considered storm events. The area coverage for this study is 650 km × 550 km, or roughly 350 000 km^2 (~130 000 mi^2). All East Coast winter storms between 1982 and 1990 that remained within this region for a period exceeding 6 h were analyzed.

Past storm trajectory information was retrieved from the North American surface weather maps obtained from the National Climatic Data Center. A 13-yr (1978–90), twice-weekly, digitized sea surface temperature (SST) dataset was used for this research. These analyses depicted regional sea surface temperatures that included the western edge of the Gulf Stream front.

Corresponding author address: Dr. Sethu Raman, Department of Marine, Earth, and Atmospheric Sciences, North Carolina State University, Box 8208, Raleigh, NC 27695-8208.
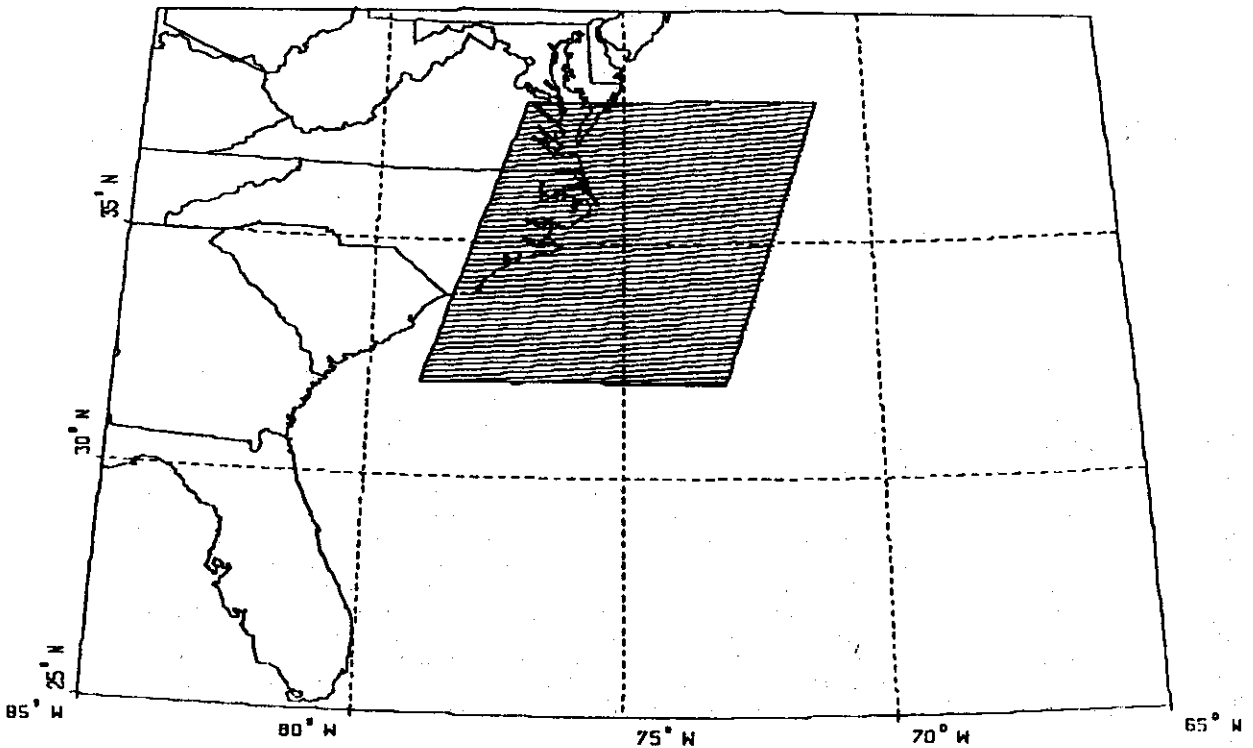
FIG. 1. Map of the eastern United States. The domain used to study East Coast winter cyclogenesis or cyclone redevelopment using climatological data is shaded in gray.

Since detailed SST data were only available 9 of these 13 years dating back to January 1982, only storms occurring after 1982 were included in this study.

In order to accomplish our research objective linking horizontal baroclinicity with cyclogenetic intensification, a reliable low-level baroclinic indicator had to be established. This indicator was devised as to quantitatively ascertain the average horizontal low-level thermal contrasts present between the GSF and the North Carolina coastline during prestorm conditions. One such measure of prestorm baroclinicity was obtained using the near-surface air temperatures at coastal locations and the corresponding SST of the Gulf Stream front. Cape Hatteras and Wilmington were the coastal observation sites used in this study. Near-surface air temperatures were obtained at 3-h intervals (over 24 h) at both locations. The air temperatures were averaged during the coldest 24 h of the prestorm period. The objective was to find a prestorm period with maximum low-level baroclinicity. After combining the averaged surface temperatures with the SST of the Gulf Stream front, the average prestorm horizontal air–sea temperature contrast was attained. Near-surface air temperature over the Gulf Stream was assumed to be the same as the observed Gulf Stream front SST. Also, SSTs were assumed to be constant throughout the 24-h period over which surface air temperature was averaged. Since the location of the western edge of the

Gulf Stream relative to the coastline was available, an average air-temperature gradient could be computed. Storm intensification was taken to be the surface central-pressure decrease, which corresponded to the pressure change experienced by a cyclone located in the study area.

As previously mentioned, the dataset included the position of the Gulf Stream's western boundary and corresponding SSTs of the area from 1 January 1982 through 30 April 1990. Since our main interest was in winter storms, the observations considered were for a 6-month time period each year from November to April.

3. Discussion of results

Over 47 winter months, 116 storms were observed. Any storm that entered or formed within the area of interest (Fig. 1) and remained within this region for more than 6 h was included in the study. Storm totals based on these data are shown in Fig. 2. This figure illustrates the distribution and shows the month with maximum storm occurrence to be January. The values in parentheses indicate the number of months observed. Storm data were not available for 5 months between January 1982 and April 1990. The five missing months were April of 1982, 1983, and 1984, and November and December of 1983.
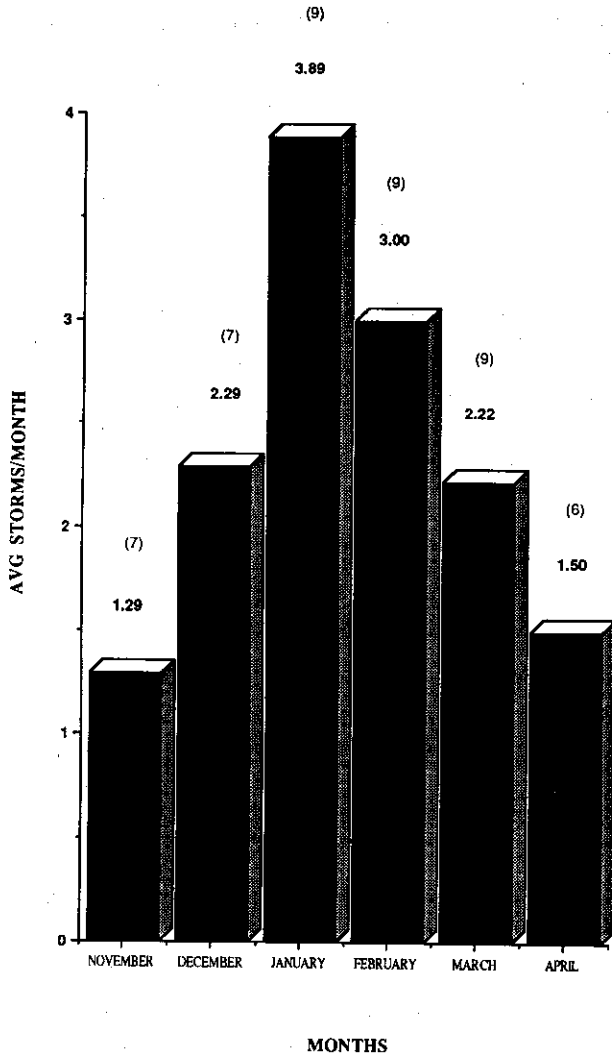
(9)

3.89

FIG. 2. Average number of storms per month with the number of months indicated in parentheses. Note the maximum number of storms observed in January.

Boundary-layer baroclinicity depends upon the horizontal gradient of air temperature. During the 9-yr period of observations, the average distance from Cape Hatteras to the GSF was approximately 65 km, while the distance from Wilmington to the GSF was nearly 195 km. Lateral meandering of the GSF makes these distances vary, such that at Hatteras the GSF varied from 15 to 120 km from the coast, while offshore of Wilmington, the front was between 100 and 300 km (Fig. 3). The horizontal temperature difference between the coast and the Gulf Stream varied from a minimum of 3°C to a maximum of 30°C.

4. Atmospheric preconditioning period

As a cyclone departs to the north and east, high pressure from the west builds into the mid-Atlantic coastal

region. Under this fairly typical scenario, strong north-to-northwesterly winds resulting from the storm are further enhanced by the circulation of the approaching anticyclone. These brisk winds can persist for up to 2 days. With such strong synoptic-scale pressure gradients, small-scale circulations that arise from local pressure gradients have little opportunity to develop. Colder air to the north and west and warm air to the south and east sets up a strong, south–north-oriented thermal wind pattern off the Carolina coast. This can be seen mathematically by the thermal-wind equation:

$$V_T = \frac{-R}{f} \int_{P_0}^{P_1} (\mathbf{k} \times \nabla T) d(\ln P), \qquad (1)$$

where R is the universal gas constant, P is the atmospheric pressure, $(\mathbf{k} \times \nabla T)$ is the curl of the thermal gradient, and f is the Coriolis parameter. The direction of the thermal gradient is toward the warmer Gulf Stream, which in turn indicates a southwesterly thermal wind. During the early stages of cold-air outbreaks, northwesterly winds at the surface turn cyclonically (back) with height, which is indicative of cold advection (see Figs. 4a,b). Furthermore, large temperature contrasts that can exist between the cold continental and relatively warm Gulf Stream environs act to strengthen the magnitude of the thermal wind and lead to the
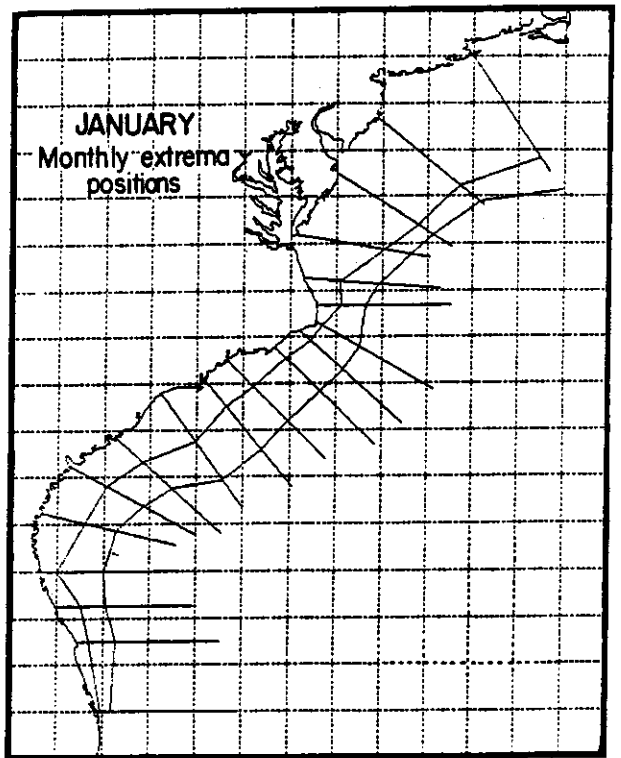

FIG. 3. The extreme positions (farthest and closest) of the Gulf Stream front (GSF) for January for the 9-yr period 1982–90. The lines eminating from the United States coastline are transects that depict horizontal distance to the GSF.
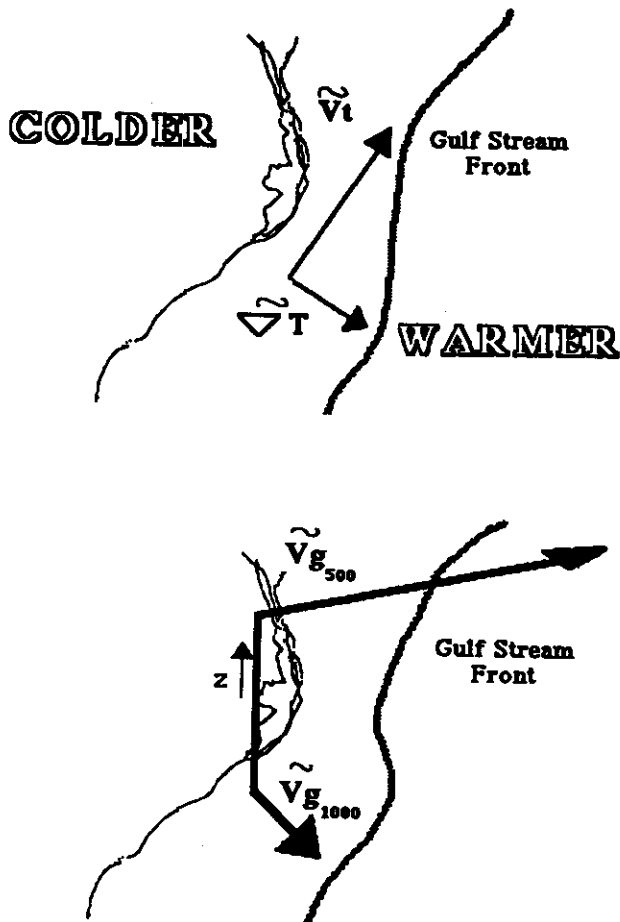
FIG. 4. (a) Schematic of the thermal-wind pattern during a typical period of cold advection. Note the cold, dry continental air mass to the north and west, while the warm, moist Gulf Stream environment is to the south and east; (b) This figure depicts the geostrophic wind V_g backing (turning cyclonically) with height, which is indicative of a cold advective pattern. Note how V_g increases in magnitude at upper levels. This increase in magnitude is proportional to the thermal wind V_t, which in turn is dependent upon the strength of the horizontal thermal gradient.

formation of a low-level jet (Uccellini et al. 1987). Initially, as the continental air mass encounters the MBL in and around the Gulf Stream, the denser, colder air displaces the relatively warm marine air, resulting in moist convection and the formation of shallow clouds over the Gulf Stream. The onset and intensity of convection and cloud formation depends on the degree of MBL modification and vertical moisture transport to the lifting condensation level (Huang and Raman 1990, 1991, 1992). The cold and dry continental air mass that advects over the midshelf and Gulf Stream regimes is continually warmed and moistened from the sea surface below, which allows the depth of the MBL to increase with time.

This time is referred to as the atmospheric preconditioning period. This "prestorm" period, which occurs during the CAO, may significantly affect the intensi-

fication of subsequent mid-Atlantic winter cyclones. The transition from CAO to either coastal cyclogenesis or storm redevelopment, however, has not been well studied. It is believed that this CAO period, which is typified by strong convection over coastal waters (especially off North Carolina and southeastern Virginia), acts to considerably warm and moisten the MBL vertically over time. In this section, attempts are made to show the approximate time scales associated with this preconditioning period.

During strong cold-air outbreak conditions, large sensible and latent heat fluxes are known to occur over Gulf Stream waters (Pietrafesa et al. 1985; Raman and Riordan 1988). It has been shown (Vukovich et al. 1991) that during moderate to strong CAOs, the largest values and strongest gradients of total heat flux exist offshore to the north and east of Cape Hatteras. This is to be expected since the region allows for very little time and distance (approximately 2–3 h assuming 20–30 km h^{-1} offshore flow) for the colder continental air mass to modify before encountering the much warmer waters offshore. Vukovich et al. (1991) described the heat-flux time histories of two strong CAOs during the Genesis of Atlantic Lows Experiment (GALE) conducted in 1986. The two specific events looked at occurred on 11–12 February 1986 and 24–25 February 1986. The respective maximum heat-flux values for these cases occurred 30 and 42 h after CAO conditions began. Wayland and Raman (1989) found similar results, whereby peak total heat-flux values were recorded after 30 h of offshore cold advection. In these cases even after 42 h, observed surface heat fluxes were roughly 70% of their maximum value. Many times, under such strong CAO conditions, substantial air–sea temperature contrasts are observed several hours (36–48) after CAO onset. The low-level, persistent wind conditions typically found during this period act in conjunction with these strong air–sea contrasts to enhance and maintain the strong surface heat-flux distribution of the region. Occasionally during wintertime CAOs, the coastal waters off North Carolina and southeastern Virginia are transformed into a region of strong surface-layer heating due to the proximity of the Gulf Stream. This area is characterized by large horizontal gradients in temperature and specific humidity, which in turn leads to large gradients in sensible and latent heating. We roughly define the coastal waters off North Carolina and southeastern Virginia as the region between the latitudes 35° and 37°N west of 72°W.

Cione (1992) has recently completed a study of rapidly intensifying cyclones [cyclones exhibiting average central-pressure decreases greater than 12 mb (12 h)$^{-1}$] between the years 1982–90. During this time period, 19 such events were observed (Fig. 5). Of these 19 occurrences, 16 had prestorm conditions typified by relatively strong horizontal, land air SST contrasts. That is, for each event, the average prestorm condition was characterized by at least a 14°C difference between

FIG. 5. The yearly frequency distribution of 19 rapidly intensifying storms $[dP/dt > 12$ mb $(12$ h$)^{-1}]$ between 1982 and 1990.

them as a function of latitude, a distinct intensification maximum occurred between 35° and 37°N (Fig. 7). This also coincides with the heat flux maxima zone described earlier that is typically observed north and east of Cape Hatteras during strong CAO conditions (Vukovich 1991; Wayland and Raman 1989).

A quantitative measure of the length and intensity of the preconditioning period was of interest. The observed coldest land air temperature (during offshore flow) for the prestorm period was recorded for each event. This would represent the time of maximum offshore contrast between air and sea. It has been observed that the time of minimum air temperature nearly coincides with the time of maximum wind speed during CAO events (Vukovich 1991). Therefore, at this time, one would expect to observe near maximum values for latent and sensible heat flux. The observed time of deepest intensification (over 3 h) for each of the 116 storms was obtained. The lag time between the occurrence of maximum air–sea temperature contrast (which coincides with the time of near maximum heating) and the time of most rapid storm intensification was investigated as well. The storms were broken into two groups: strong storms [central-pressure decreases over time $dP/dt > 12$ mb $(12$ h$)^{-1}]$ of which there were 19, and all other events, of which there were 97. The weaker storm group exhibited an average lag time of 41.2 h with a standard deviation of 17.7 h, while the stronger events' average lag time was 20.8 h. The standard deviation for this group was 11.4 h. A standard t test showed that the difference between means was statistically significant beyond the 1% level. In Fig. 8, the DIP range is compared with the average lag times for all events. Note the inverse relationship present between the period of maximum intensification and the lag time. The "high-DIP" storms entered the offshore region during periods of moderate to strong upward heat and moisture flux. This, in part, may explain why these lower lag-time storms experienced such deep regional intensification. It is also worth noting that the apparent phase lag present between maximum low-level heating and deepest intensification is somewhat reduced when we consider that a large percentage of the maximum total heat flux occurring during strong CAOs is often observed well after the onset of cold advection (Vukovich 1991; Wayland and Raman 1989). In some instances, rather significant values of surface heat and moisture flux can be found within the offshore Carolina region beyond 48 h of CAO onset.

Gyakum (1983) observed that low-level surface heating, especially latent heating, can enhance the process of rapid offshore cyclonic development. Gyakum showed how significant variations in latent heating could substantially affect (up to 25%) the rate of cyclonic intensification during the rapid development phase. Large variations of latent, as well as total low-level heat flux, exist offshore North Carolina and southeast Virginia during strong CAO periods. Low-

the averaged coastal land air temperature (over 24 h) and the SST of the Gulf Stream front. The average contrast for these 16 events was 21°C. The tracks and central pressures of these storms were observed over 3-h increments, which made it possible to ascertain a deepest intensification period (DIP) for each cyclonic event. Among the 19 strong-storm events, a relationship existed between the magnitude of the prestorm CAO period and the observed DIP. Statistical analysis yielded a significant correlation coefficient of 0.59 between the two variables. After examining the tracks and DIPs for all 19 events, a pattern seemed to emerge. For 16 of the 19 storms (~85%), DIPs occurred within a region west of 72° between the latitudes of 34° and 37°N. The average storm track, Gulf Stream frontal position, and DIP value for these 16 storms are shown in Fig. 6. After averaging the various intensification rates (over 3 h) from these 16 storms and displaying
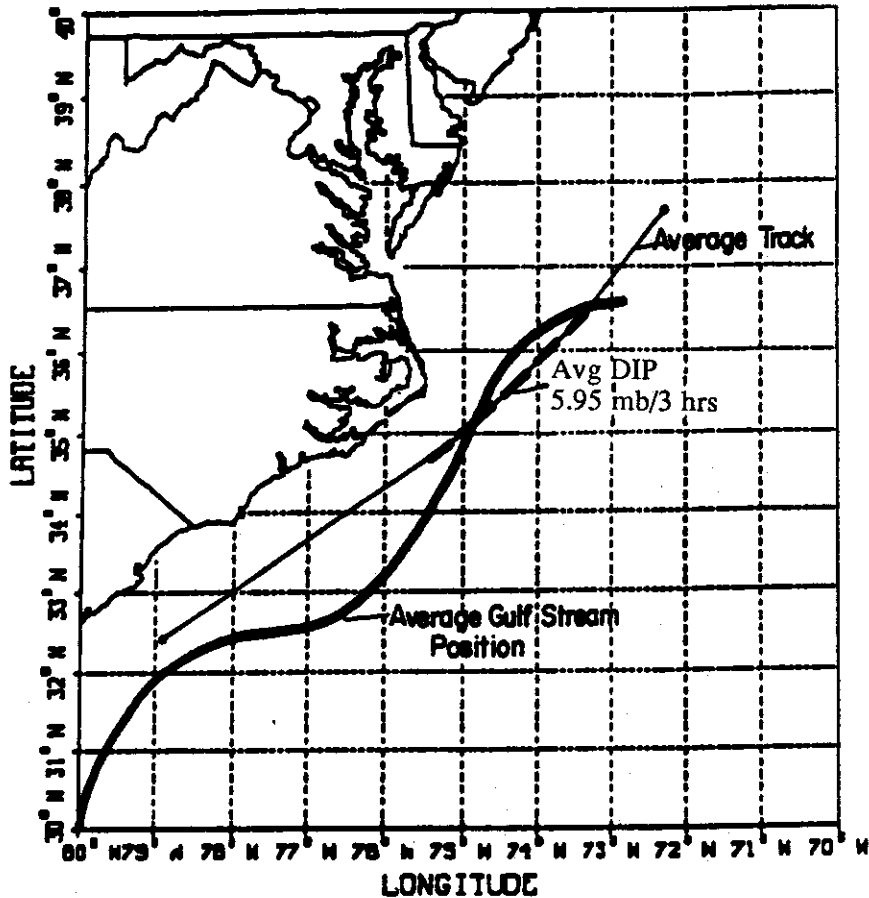
FIG. 6. The average storm track, Gulf Stream position, and deepest
intensifying period (DIP) for 16 of the 19 events shown in Fig. 5.

level heat-flux distributions within this region can vary quite significantly, even over small periods of time. For example, during strong offshore cold advection, the distribution of total surface heat flux approximately 20 h after the time of maximum low-level heating is much greater in magnitude and areal coverage when compared to a distribution covering the same regime approximately 40 h after the time of maximum surface heat flux (Vukovich et al. 1991; Wayland and Raman 1989). In this section, it has been shown that the stronger storms are associated with much smaller lag times when compared to the weaker events. As previously noted, a sizeable percentage of the peak total heat flux that occurs during strong CAO events can exist 12 h or more after the time of maximum total heat flux. Therefore, the disturbances characterized by significantly smaller lag times may have entered a region of relatively high surface-layer heating.

It has also been observed in some instances that surface fluxes do not play a major role during the rapid storm development stage (Kuo et al. 1990). In these cases, it has been observed that the largest flux values occur in the rear, or cold advective quadrant, of the storm. It is argued that these low-level surface fluxes would not help to intensify the existing cyclone. Many times this may be the case. Sixteen out of the 19 total strong storms alluded to in this research, however, exhibited relatively small lag times (~20 h) when compared to the 97 weaker events (~40 h). In these rare instances, the developing cyclone can utilize the potentially significant surface fluxes of the region.

Many of the 19 rapidly intensifying events entered the study domain (Fig. 1) during an offshore flow pattern that would allow the region to maintain a relatively high level of horizontal low-level baroclinicity. Rogers and Bosart (1986) and Nuss and Anthes (1987) showed how low-level baroclinic instability can rapidly transform a shallow, lower-tropospheric oceanic disturbance into a deep vortex that is very apparent at mid- and upper levels. Rogers and Bosart (1986) looked at a rapidly intensifying oceanic cyclone and showed how baroclinic instability led to deep cumulus convection within central regions of the storm. It was found that the latent-heat release associated with this deep cumulus convection acted to decrease the central surface pressure quite substantially, which then increased the
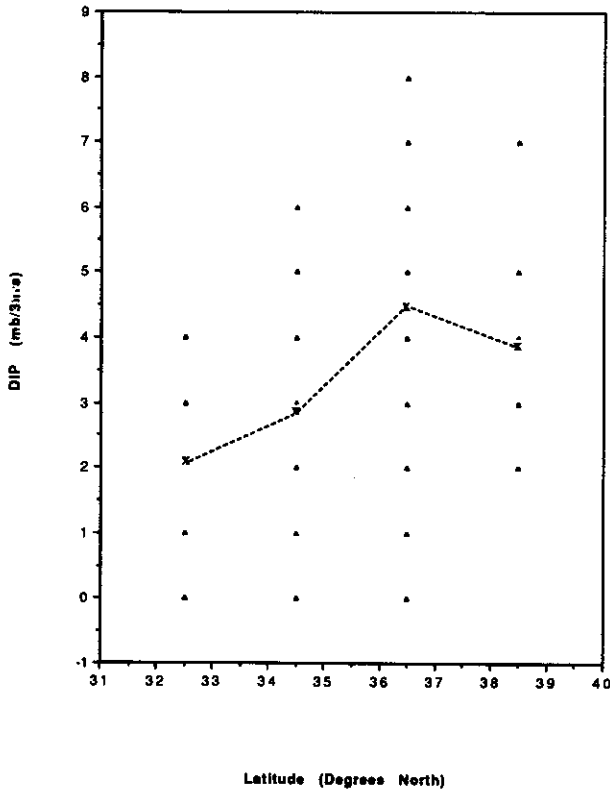
FIG. 7. The intensification rate as a function of latitude for 16 rapidly intensifying cyclones. Four regions of intensification (31.5°–33.5°N; 33.5°–35.5°N; 35.5°–37.5°N; 37.5°–39.5°N) were analyzed. Triangles depict the distribution of observed DIPs for these 16 storms, while the X's represent the average DIP for each of the four zones. Note that in some instances triangles represent more than one observation.

low-level wind field and convergence pattern of the developing system.

In summary, the lag times associated with the intense cyclones are significantly lower than those of weaker disturbances. For the decreased lag time condition, the region will 1) remain highly baroclinic at low levels (especially if the flow pattern retains a northerly component), and 2) still show signs of a strong offshore heat-flux distribution. Also, the magnitude of the prestorm CAO is substantially larger for these stronger storms when compared to the weaker events [21.0°C (strong) vs 12.2°C (weak)]. In fact, even among the 19 strong-storm events, a relationship existed between the magnitude of the prestorm CAO period and the observed DIP. Statistical analysis yielded a significant correlation coefficient of 0.59 between the two variables. It was also observed that 85% of the strong storms intensified within a narrow, highly baroclinic region off North Carolina and southeastern Virginia. This zone of intense deepening also coincides with the region of maximum low-level offshore heating and vertical moisture transport (during strong CAO conditions). The fact that a large percentage of these stronger storms

deepened in roughly the same maximum heat-flux region, experienced much smaller lag times, and were typified by large prestorm air–sea temperature contrasts, seems to indicate that the highly baroclinic conditions present offshore North Carolina and southeast Virginia during the prestorm and development stages acted to significantly affect the local intensification rates of these events.

5. Gulf Stream position

One of the points of interest of this study is to test the hypothesis that storm intensification is influenced by the Gulf Stream's relative location with respect to the North Carolina coast. One possible way to accomplish this is by combining the climatological history of the Gulf Stream position with the past history of cyclonic events that occurred within our experimental domain. We divided the 116 documented storm events into two subgroups. One group (A) contained storms that experienced pressure drops $dP/dt > 12$ mb (12 h)$^{-1}$, while the other group (B) was entirely composed of disturbances with pressure decreases less than or
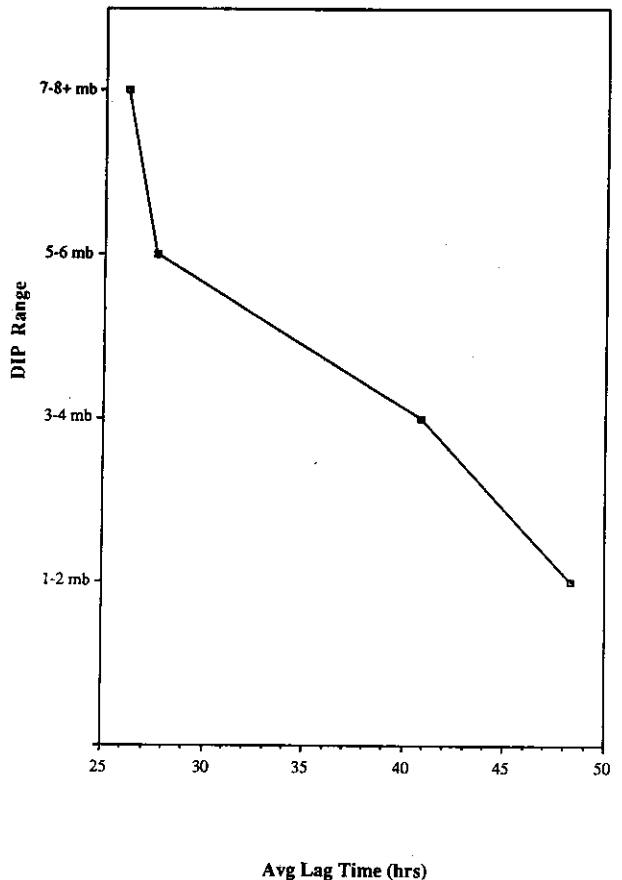

Avg Lag Time (hrs)

FIG. 8. The DIP range versus the average lag time. Here, lag times were averaged for events that had DIPs of 1–2 mb (3 h)$^{-1}$, 2–3 mb (3 h)$^{-1}$, etc.

equal to 12 mb $(12 \text{ h})^{-1}$. For the 19 group-A storms at Cape Hatteras, it was found that the mean distance to the Gulf Stream's edge was 56.6 km, with a standard deviation of 17.1 km. For the 97 group-B storms, the observed mean and standard deviation were 71.4 and 26.8 km, respectively. Using a two-sample t test that assumed unequal variance, a true difference between means was found well beyond the 0.5% significance level. The same analysis was undertaken for the distance data at Wilmington. For group A, we saw the average distance and the standard deviation to be 194.6 and 33.1 km, respectively. For group B, a mean value of 192.8 km with an average standard deviation of 30.2 km was found to be the case. Unlike the Cape Hatteras data, however, no true difference between means could be established at either the 1%, 5%, or 10% level. We also constructed a 95% confidence interval for $[y \text{ avg}(1) - y \text{ avg}(2)]$, where $y \text{ avg}(1)$ is the mean distance for the stronger storms, while $y \text{ avg}(2)$ represents the average for weaker storms. Our upper and lower 5% bounds for the difference between these two averages turned out to be −6.2 and −21.2 km, respectively. That is, with 95% certainty, a true difference between the means exists within this range. The corresponding 99% range is −3.0 and −24.4 km.

These results suggest that the Gulf Stream position may indeed affect initial deepening rates since the Gulf Stream to Hatteras prestorm distance is clearly less during subsequent periods of deep offshore intensification. The fact that no relationship was found between the Wilmington distance to the Gulf Stream front and subsequent deepening rates may indicate that the Wilmington distance is simply too large. This increased GSF-to-land distance would undoubtedly allow for enhanced continental airmass modification by near coastal and offshore waters during periods of offshore cold advection (Wayland and Raman 1988). With a typical Gulf Stream distance of 65 km, a modest and steady 20 km h^{-1} offshore wind would roughly travel 3 h from Hatteras before reaching the Gulf Stream frontal zone, while the flow off Wilmington would take nearly 10 h. Thus, it is possible that the extended period of airmass modification experienced by the Wilmington case does indeed temper the relative magnitude of the low-level horizontal baroclinicity. This would help to explain why a strong relationship was found between the Gulf Stream distance and the rate of initial deepening at Cape Hatteras. The standard deviations of the Gulf Stream distances for the four subgroups are as follows: strong storms at Hatteras, weaker storms at Hatteras, strong storms at Wilmington, and weaker storms at Wilmington were 17.1, 26.8, 33.1, and 30.2 km, respectively. Of these, the one result that stands out is the value of 17.1 km. This smaller standard deviation at Cape Hatteras for storms experiencing pressure drops greater than 3 mb $(3 \text{ h})^{-1}$ may suggest a "preferred" position of the Gulf Stream front with regard to deep intensification or cyclogenesis.

To further investigate the findings linking Gulf Stream location with subsequent deepening, it was decided to observe the entire time history of Gulf Stream position over a more continuous time scale. The entire dataset analyzed consisted of 47 months from January 1982 through April 1990. As mentioned earlier, only the winter month period of 1 November–30 April was included in this research. There were a total of 194 Gulf Stream positions that encompassed a 194-week period. These observations correspond to one per week. Over this entire time history, Hatteras had an average Gulf Stream distance of 68.2 km with a standard deviation of 25.8 km. For Wilmington, the average was 191.8 km and the standard deviation was 32.8 km.

An attempt was made to see if there was a significant difference in the mean position of the Gulf Stream front off Cape Hatteras during various meteorological conditions. In this section, strong cyclonic dates were compared with all other Gulf Stream position dates. Eliminating the times for which we had no opportunity, for one reason or another, to observe meteorological activity, the dataset was reduced to 166. We then eliminated days associated with strong cyclogenetic activity [i.e., strong storms with $dP/dt > 12 \text{ mb } (12 \text{ h})^{-1}$ (19 events)]. From the remaining 147 dates, Cape Hatteras was found to have an average distance of 70.5 km and a standard deviation of 27.6 km. As already mentioned, the 19 strong cyclonic dates had a mean and standard deviation of 56.6 and 17.1 km, respectively. Again, using a two-sample t test, a statistically significant difference ($\sim$0.5% level) between the mean distance of the strong dates (19) and the mean distance of all other Gulf Stream position dates (147) was observed. Similar analyses were undertaken using data at Wilmington, but statistically significant results were not found.

6. Thermal gradients

One of the relationships of interest is the temporal variation of central pressure versus the horizontal thermal gradient. The thermal gradient is obtained by combining both the prestorm low-level horizontal temperature contrast and the prestorm horizontal distance between the GSF and the two coastal sites at Cape Hatteras and Wilmington. This horizontal thermal gradient is a good indicator of low-level MBL baroclinicity since it takes into account the temperature contrast between the coastal and offshore locations as well as the distance present between them. Multiple linear regression analyses were conducted using prestorm temperature contrasts and distances as predictors for observed central-pressure decreases for the 116 cyclones studied. Table 1 summarizes the regression analyses results for Cape Hatteras and Wilmington.

For the Cape Hatteras thermal-gradient model, both the prestorm horizontal temperature difference and the GSF-to-land distance contributed to the explained variance R^2. For both model analyses, the temperature difference independent variable is highly significant (denoted by the very low probability greater than F

TABLE 1. Summary of multiple linear regression analysis.

Variable/model	Model rms error [mb $(12\ h^{-1})$]	F ratio	Probability $> F$	Model $R^2(R)$
Cape Hatteras to GSF horizontal temperature difference (°C)	—	86.7	>0.01%	—
Cape Hatteras to GSF horizontal distance (km)	—	3.8	5.4%	—
Cape Hatteras thermal-gradient statistical model	3.5	43.4	>0.01%	.450(.671)
Wilmington to GSF horizontal temperature difference (°C)	—	68.4	>0.01%	—
Wilmington to GSF horizontal distance (km)	—	0.9	34.6%	—
Wilmington thermal-gradient statistical model	3.7	34.3	>0.01%	.395(.628)

value) and is the dominant factor that contributes to the explained variance. If, however, the Hatteras analysis is completed without including the GSF-to-Hatteras distance parameter, the resulting R^2 is reduced to 0.430, while the rms error increases to 3.6 mb (12 h)$^{-1}$. For the Wilmington model, this is not the case. In fact, the explained variance actually decreases to 0.389 when the GSF-to-Wilmington distance is introduced into the analysis. These results, which show the GSF-to-Wilmington (Hatteras) distance to be statistically insignificant (significant), agree with the findings presented in section 5. The competing processes involved with central-pressure decrease (upper-level dynamics, storm track, specific low-level conditions during development stages, etc.) along with the sampling time differences that exist between Gulf Stream positioning and land air-temperature-averaging procedures are the major factors affecting the degree of scatter present in Figs. 9a and 9b. These figures show regression model results that compare observed dP/dt's for all storm events (y axis) with predicted dP/dt values (x axis).

7. Conclusions

For many years, predicting offshore rapid cyclonic intensification has been a difficult problem for operational meteorologists since these events predominantly took place over the data-sparse regions covering the Atlantic. As a result, forecasters have had a limited number of tools at their disposal when assessing the potential magnitude of cyclonic development. A climatological analysis was undertaken to look into the possible effects that low-level baroclinicity induced by the Gulf Stream may have on the observed deepening rates of mid-Atlantic offshore cyclones.

Many have shown that the Gulf Stream meanders appreciably due to its own dynamics (Pietrafesa et al. 1978; Rooney et al. 1978; Brooks and Bane 1978). If the distance between the Gulf Stream and the coastline is to decrease as a result of these meanders, the net effect would be an increased baroclinic MBL. This increased low-level baroclinicity may eventually affect the degree of offshore development of succeeding cyclones. When the prestorm Cape Hatteras-to-Gulf Stream distances of strong cyclonic events [$dP/dt > 12$ mb (12 h)$^{-1}$] were compared with weaker events [$dP/dt < 12$ mb (12 h)$^{-1}$], it became clear that these more

intense events were characterized by significantly smaller GSF-to-land distances (56.6 vs 71.4 km). The same results were found when the Cape Hatteras-to-Gulf Stream distances of rapidly deepening events were compared with Cape Hatteras-to-Gulf Stream distances for all other time periods.

The multiple linear regression analysis involving central-pressure decrease with the horizontal temperature distribution indicated a rather good relationship. The multivariate analysis at Hatteras showed how both the GSF distance and prestorm temperature difference was associated with the subsequent rate of offshore cyclonic intensification. The competing processes involved with central-pressure decrease, along with sampling time differences present between Gulf Stream positioning and land air-temperature-averaging procedures are probably the major factors affecting the degree of scatter observed in Figs. 9a and 9b. Nevertheless, the relationships given do show that the prestorm low-level baroclinic nature of this region plays a key role in the eventual intensification of cyclonic events entering the study domain.

The deepest intensification period (DIP), like dP/dt, represents a quantitative measure of storm intensification. Here, however, the units of the DIP are measured in millibars per 3 hours, which gives a more localized, smaller scale (in time as well as space) representation of cyclonic intensification. In this study, 85% (16/19) of the strong storms experienced their DIP within a narrow offshore region between 34° and 37°N, west of 72°. During conditions of strong offshore cold advection, this region coincides with an area typified by large gradients in total heat flux. Comparing the magnitudes of the prestorm CAOs for weak and strong events, it was observed that the stronger storms had an average prestorm horizontal thermal contrast [GSF(SST) − 24-h-averaged land air temperature] of 21°C, while the weaker events experienced a contrast of only 12.2°C. The strong storms also experienced average lag times of roughly 20 h, while the weaker events average lag time was more than 40 h. This decreased lag time allows much of the region depicted in Fig. 1 to remain baroclinically unstable. It is also probably true at this juncture that much of the offshore region (especially between 34° and 37°N, west of 72°) still maintains a moderate to strong horizontal surface heat-flux distribution. If we combine all these factors, it becomes increasingly apparent that the region off-

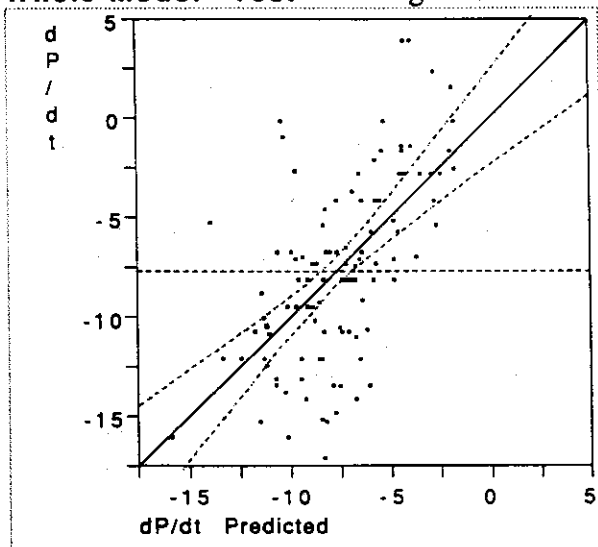## Whole-Model Test Cape Hatteras
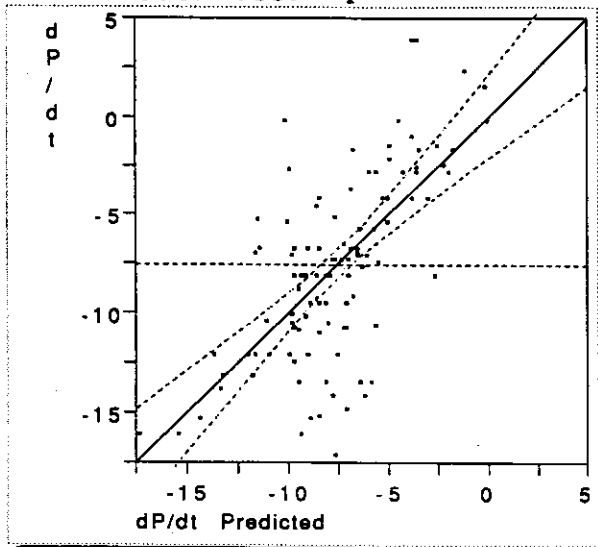
Whole-Model Test Wilmington

FIG. 9a. The Hatteras statistical model compares the observed dP/dt (y axis) with the predicted dP/dt (x axis) for the 116 storms. The independent variables used in the analysis are the prestorm low-level temperature contrast between the GSF and Cape Hatteras and the prestorm horizontal distance from the GSF to Cape Hatteras. (b) The Wilmington statistical model compares the observed dP/dt (y axis) with the predicted dP/dt (x axis) for the 116 storms. The independent variables used in the analysis are the prestorm low-level temperature contrast between the GSF and Wilmington and the prestorm horizontal distance from the GSF to Wilmington.

shore southeast Virginia and northeast North Carolina is potentially a maximum intensification zone for developing cyclones south of 38°N.

REFERENCES

Bosart, L. F., 1981: The Presidents' Day snowstorm of 18–19 February 1979: A subsynoptic-scale event. *Mon. Wea. Rev.*, **109**, 1542–1566.
——, C. J. Vaudo, and H. J. Helsdon, Jr., 1972: Coastal frontogenesis. *J. Appl. Meteor.*, **11**, 1236–1258.
Brooks, D. A., and J. M. Bane, 1978: Gulf Stream deflection by a bottom feature off Charleston, South Carolina. *Science*, **201**, 1225–1226.
Cione, J. J., 1992: The effects of surface forcing on mid-Atlantic winter cyclones. M.S. thesis, Department of Marine, Earth, and Atmospheric Sciences, North Carolina State University, 120 pp.
Gyakum, J. R., 1983: On the evolution of the *QE II* storm. Part II: Dynamic and thermodynamic structure. *Mon. Wea. Rev.*, **111**, 1156–1173.
Holt, T., and S. Raman, 1990: Marine boundary-layer structure and circulation in the region of offshore re-development of a cyclone during GALE. *Mon. Wea. Rev.*, **118**, 392–410.
Huang, C. Y., and S. Raman, 1990: Numerical simulations of cold air advection over the Appalachian mountains and the Gulf Stream. *Mon. Wea. Rev.*, **118**, 343–361.
——, and ——, 1991: Numerical simulation of January 28 cold air outbreak during GALE. Part II: The mesoscale circulation and the marine boundary layer. *Bound.-Layer Meteor.*, in press.
——, and ——, 1992: A three-dimensional numerical investigation of North Carolina coastal front and the Gulf Stream rainband. *J. Atmos. Sci.*, **49**, 560–584.
Kuo, Y. H., R. J. Reed, and S. Low-Nam, 1990: Effects of surface energy fluxes during the early development and rapid intensification stages of seven explosive cyclones in the Western Atlantic. *Mon. Wea. Rev.*, **119**, 457–476.
Nuss, W. A., and R. A. Anthes, 1987: A numerical investigation of low-level processes in rapid cyclogenesis. *Mon. Wea. Rev.*, **115**, 2728–2743.
Pietrafesa, L. J., L. P. Atkinson, and J. O. Blanton, 1978: Evidence for deflection of the Gulf Stream by the Charleston rise. *Gulfstream*, vol. IV, no. 9, 3–7.
——, G. S. Janowitz, and J. Whittman, 1985: Physical oceanographic processes in the Carolina Capes. *Coastal and Estuarine Sciences*, **2**, 23–33.
Raman, S., and A. J. Riordan, 1988: The Genesis of Atlantic Lows Experiment: The planetary-boundary-layer subprogram of GALE. *Bull. Amer. Meteor. Soc.*, **69**, 161–172.
Rogers, E., and L. F. Bosart, 1986: An investigation of explosively deepening oceanic cyclones. *Mon. Wea. Rev.*, **114**, 702–718.
Rooney, D. M., G. S. Janowitz, and L. J. Pietrafesa, 1978: A simple model of the deflection of the Gulf Stream by the Charleston rise. *Gulfstream*, vol. IV, No. 11, 2–7.
Sanders, F. J., and J. R. Gyakum, 1980: Synoptic-dynamic climatology of the "bomb." *Mon. Wea. Rev.*, **108**, 1589–1606.
Uccellini, L. W., R. A. Petersen, K. F. Brill, P. J. Kocin, and J. J. Tucillo, 1987: Synergistic interaction between an upper-level jet streak and diabatic processes that influence the development of a low-level jet and a secondary coastal cyclone. *Mon. Wea. Rev.*, **115**, 2222–2261.
Vukovich, F. M., J. W. Dunn, and B. W. Crissman, 1991: Aspects of the evolution of the marine boundary layer during cold-air outbreaks off the southeast coast of the United States. *Mon. Wea. Rev.*, **119**, 2252–2278.
Wayland, R., and S. Raman, 1989: Mean and turbulent structure of a baroclinic marine boundary-layer during the 28 January 1986 cold air outbreak (GALE86). *Bound.-Layer Meteor.*, **48**, 227–254.